Effect of Array Configurations on the Performance of GNSS Interference Suppression

Chung-Liang Chang and Jyh-Ching Juang*

Abstract: This paper analyzes, through simulations, GNSS interference mitigation performance against wideband and narrowband interferences by using spatial-temporal adaptive processing (STAP). The mathematical analysis results demonstrate that the array configuration has a considerable effect on the spatial-temporal correlation function. Based on the results, different array configurations are presented to evaluate and observe the effect on interference mitigation. The analysis results are further assessed through simulations.

Keywords: Antenna array, GNSS, interference mitigation, STAP.

1. INTRODUCTION

In recent years, the Global Navigation Satellite System (GNSS) has been widely used in military and civilian application to provide users with information of position, velocity, and time. Although the Global Positioning System (GPS) system offers some inherent anti-jam protection [1,2], owing to its low signal power from satellite, an interfering signal with enough power and a time/frequency signature could adversely affect the use of GPS signal for navigation [3]. It is necessary to suppress the interference well below the weak GPS signal.

Throughout the years, many interference mitigation techniques of GPS have been developed; see, e.g., [4-11]. However, these approaches [4-7] may be effective against a certain type of interferences, but may not be applicable to all jammers. The traditional adaptive antenna techniques [8-11] may ultimately run out of degree of freedom as the number of interferences increases and may be inadequate for wideband operation.

Recently, the spatial-temporal adaptive processing (STAP) techniques have been applied to perform 2D (spatial and temporal domain) filtering on GPS signals so as to eliminate narrowband and broadband/co-channel interferences [12-15]. Most of the adaptive array algorithms function along with different array configurations to proceed with interference mitigation analysis, such as Uniform Linear Array (ULA) in [14], Uniform Circular Array (UCA) in [10,12,13,15], and Uniform Rectangular Array (URA) in [9,11,16]. However, the performance of the adaptive antennas is susceptible to several factors, among which array configuration is an essential one, as is mentioned in [17].

In the traditional antenna systems, array configuration consisting of array aperture, array elements' locations and individual element pattern clearly illustrates the characteristics of the associated steering vectors, or the array manifold. For traditional narrowband adaptive antennas, spatial correlation coefficients play a prominent part in the output performance [18]. The smaller the spatial correlation between the desired and interference sources, the better the output performance. Similar to the performance analysis of the conventional adaptive antennas, the STAP performance is also influenced by the configuration of the employed antenna array [19,20].

In this paper, we present the notion of spatial-temporal correlation function, which adequately portrays the joint spatial and temporal correlation relationship between the desired user signal and the interference signals, as well as the influence of the array configuration on the output performance of STAP systems. Under the minimum mean square error (MMSE) criterion, an analytical form of the residual error power of array systems is obtained. We aim to analyze and compare various array configuration effects on the associated spatial-temporal correlation function in interfered environ-ment. Three general types of equally spaced arrays are considered in this paper-ULA, URA, and UCA on the associated spatial-temporal correlation function in an interfered environment. The analysis results show that the array

Manuscript received July 19, 2007; revised February 26, 2008; accepted June 16, 2008. Recommended by Editorial Board member Dong-Ho Cho under the direction of Editor Hyun Seok Yang. This work was supported by the National Science Council of Taiwan under grant NSC-96-2628-E-006-246-MY2.

Chung-Liang Chang and Jyh-Ching Juang are with the Department of Electrical Engineering, National Cheng Kung University, No. 1, University Road, Tainan 70101, Taiwan (e-mails: ngj567.liang@msa.hinet.net, juang@mail.ncku.edu.tw).
* Corresponding author.

configuration has a significant effect on the associated spatial-temporal correlation functions. The non-blind array algorithm as a method to effectively mitigate interferences is also presented. The design and analysis results shall shed light on the use of antenna array for GPS interference mitigation and multipath attenuation.

The remainder of this paper is organized as follows. Section 2 gives a description of the GPS signal model. It also briefly reviews various types of antenna array configurations. Section 3 describes the antenna array manifold vector model and the array configurations that affect system performance. The residual error power based on MMSE criterion of STAP system is evaluated. The algorithm for adaptive spatial-temporal processing is also presented in the above section. In Section 4, computer simulation results are provided under a given interfered environment to show the effectiveness of various array configurations. Finally, a short summary follows in Section 5.

2. SIGNAL MODEL

In this section, the signal model in antenna array processing is described. The GPS utilizes spread-spectrum (SS) techniques with two carriers: L1 (1575.42 MHz) and L2 (1227.6 MHz) modulated by binary navigation data and pseudorandom noise (PRN) codes. The PRN code used for GPS contains coarse acquisition (C/A) code and precision (P) code. The C/A code has a rate of 1.023 Mchip/s with a period of 1023 chips (1ms) and the P-code truncated period is one week with chipping rate of 10.23 Mchip/s. The receiver can calculate its position and time by measuring the distance to the satellites (at least four) in relation to X, Y, Z, and receiver timing, respectively, so as to calculate position-velocity-time (PVT) solution. The GPS navigation data is transmitted at an information bit rate of 50 bit/s. The received antenna signal is RF filtered and down-converted to IF, then sampled and quantized. The quantized signal is then fed to the code and carrier-tracking loops. The received GPS signal power from the satellites is extremely weak because of the long distance to the satellites. The signals are actually far below the thermal noise floor according to the spectrum-spreading property. In GPS operation when the receiver is on the ground, the input signal-to-noise ratio (*SNR*) value depends on RF-bandwidth of the receiver front-end and is typically around -20dB (2MHz C/A code bandwidth). Assume that blocking within the radio front-end resulting in reduced gain and intermodulation can be mitigated through STAP or be ignored. The ideal received signal is composed of the GPS signal, background noise, thermal noise and a variety of interferences. The received baseband signal at time instant k of N antenna element with M tapped delay-line can be described by an $NM\times 1$ vector as follows:

$$\mathbf{x}(k)=\sqrt{P_s}\mathbf{A}\mathbf{s}(k)+\sum_{j=1}^{J}\sqrt{P_j}\mathbf{B}_j\mathbf{i}_j(k)+\mathrm{C}(k), \tag{1}$$

where $\mathbf{x}(k)=\left[x_{11}(k)\cdots x_{N1}(k)\ x_{12}(k)\cdots x_{N2}(k)\ \cdots\ x_{1M}(k)\cdots x_{NM}(k)\right]^H$, M is the tap delay-line number of each antenna, $(\bullet)^H$ denotes the Hermitian transpose operator, $\mathbf{A}=\mathbf{I}_{M\times M}\otimes\mathbf{a}_{\varphi_s,\theta_s}$ and $\mathbf{s}(k)=\left[s(k)\ s(k-1)\cdots s\left(k-(M-1)\right)\right]^H$, $\mathbf{B}_j=\mathbf{I}_{M\times M}\otimes\mathbf{a}^{(\ell)}_{\varphi_j,\theta_j}$ and $\mathbf{i}_j(k)$ have the same structure as $\mathbf{s}(k)$, J is the total number of interfering signals, $\otimes$ denotes the Kronecker product; $\mathbf{C}(k)$ is zero-mean, temporally and spatially white noise with variance $\sigma_{\mathrm{n}}^2\mathbf{I}$. Assume that each interference can be modeled as one of three types as follows: (1) continuous wave $\cos(2\pi f_j k\mathrm{T}_s+\psi_j)$, where the f_j and ψ_j are the interference frequency and phase, respectively. T_s is the sampling inter-val, (2) wideband cyclostationary signal or co-channel interference. GPS signal is denoted by $s(k)$ which is essential modulated C/A code that is subject to data modulation, time delay, Doppler shift, and phase variation that uncorrelate with the channel noise vector. P_s and P_j are signal power and j-th interference power, respectively. $\mathbf{a}_{\varphi_s,\theta_s}$ and $\mathbf{a}^{(\ell)}_{\varphi_j,\theta_j}$ denote the $N\times 1$ steering vector with respect to GPS satellite and j-th interfering source, respectively.

Two signal condition characterization measures are considered; the input interference-to-noise ratio is given by

$$\mathrm{INR}=10log_{10}\frac{\mathrm{P_j}}{\sigma_{\mathrm{n}}^2}, \tag{2}$$

the input signal-to-noise ratio is given by

$$\mathrm{SNR}=10log_{10}\frac{\mathrm{P_s}}{\sigma_{\mathrm{n}}^2}, \tag{3}$$

where the input noise variance σ_{n}^2 is depicted in (1). In the following, we mainly address the problem regarding the effect of various types of antenna array configuration on interference mitigation techniques.

3. PROBLEM FORMULATION

3.1. STAP technique

In this section we investigate an adaptive spatial-temporal processing for GPS interference mitigation. The guideline in designing adaptive antenna algorithm

can be imposed in spatial domain or temporal domain. One class of these algorithms is the non-blind adaptive algorithm in which a training signal is used to adjust the array weight vector. Another technique is to use a blind adaptive algorithm which does not require a training signal. Still another is semi-blind adaptive algorithm in which the desired signal information can be obtained by inertia navigation system. In this section, a general non-blind adaptive algorithm based on conventional least-squares solution [20] is investigated for the weight coefficients of antenna array. The output of the STAP system is:

$$y(k) = \mathbf{w}^H \mathbf{x}(k), \tag{4}$$

where $\mathbf{w}$ denotes the spatial-temporal weight vector and can be described as

$$\begin{aligned}\mathbf{w}(k) = &[w_{11}(k) \cdots w_{N1}(k)\ w_{12}(k) \cdots w_{N2}(k) \\ &\cdots w_{1M}(k) \cdots w_{NM}(k)]^H .\end{aligned} \tag{5}$$

In this case, both $\mathbf{w}$ and $\mathbf{x}(k)$ are $NM \times 1$ column vectors. Under the minimum mean square error criterion, the optimal weights of STAP system is the attempt to minimize the cost function

$$J(k) = E\left\{\left\|d(k-\tau) - y(k)\right\|^2\right\}, \tag{6}$$

where $d(k-\tau)$ denotes the local replica, and $\tau \geq 0$ is the delay sample that is selected to output the best performance. $E\{\cdot\}$, is the expectation value, and $\|\cdot\|$ denotes a Euclidean norm of a vector. The optimal adaptive weights computed through the adaptive array algorithms are multiplied by each corresponding measurement data and summed up altogether to give the output for acquisition/tracking modules. The optimal weight vector, $\mathbf{w}_{opt}$, that maximizes the signal to interference plus noise ratio (*SINR*), satisfies the matrix Weiner-Hopf [20]

$$\mathbf{w}_{opt} = \mathbf{M}^{-1}\mathbf{r}_{dx}, \tag{7}$$

where $\mathbf{M} \in C^{NM \times NM}$ is the signal plus interference plus noise auto-correlation matrix, which is guaranteed to be positive definite and $\mathbf{r}_{dx} \in C^{NM}$ is cross-correlation vector.

In practice, the auto-correlation matrix $\mathbf{M}$ in (7) cannot be known a priori since it counts on the signal environment. Due to the unknown statistics of the interference, $\mathbf{M}$ must be determined adaptively from the data, which is thus mathematically equivalent to substituting sample estimate $\hat{\mathbf{M}}$ in (8) for $\mathbf{M}$.

$$\hat{\mathbf{M}}(k) = \frac{1}{L}\mathbf{X}(k)\mathbf{X}^H(k), \tag{8}$$

and the cross-correlation vector is computed as

$$\hat{\mathbf{r}}_{dx}(k) = \frac{1}{L}\mathbf{X}(k)\mathbf{d}(k-\tau), \tag{9}$$

where $\mathbf{X}(k) = [\mathbf{x}(1+kL)], \mathbf{x}(2+kL), \cdots, \mathbf{x}(k+1)L], k = 0,1,\cdots, K$, denotes the input data block which contains L snapshots of the input data vector and is used in the kth iteration. Where K is the number of iterations required for the algorithm to converge, and $\mathbf{d}(k-\tau)$ is the local replica data vector. The estimate weight vector can also be written as

$$\mathbf{w}(k+1) = \hat{\mathbf{M}}^{-1}(k)\hat{\mathbf{r}}_{dx}(k) \tag{10}$$

Some may find that equation (10) is very similar to (7). However, in (10), $\hat{\mathbf{M}}(k)$ is an estimate of the correlation matrix of the input data vector, computed over the kth data block containing L snapshots of the input data vector, and $\hat{\mathbf{r}}_{dx}(k)$ is an estimate of the cross-correlation between the local replica and input data vector. It is called time coherent block adaptive beamforming [9,16] and the new weight vector is updated in accordance with

$$\mathbf{w}(k) = \mu\mathbf{w}(k-1) + (1-\mu)\mathbf{w}(k), \tag{11}$$

where μ is a variable between 0 and 1 that is chosen to minimize the output variance $\left|\mathbf{w}^H\mathbf{M}\mathbf{w}\right|$. It is assumed that the angle of arrival (AOA) of GPS signal inside the received data is known exactly. Therefore, with an attempt to increase the speed of antenna array weight coefficients to converge, the initial weights can be obtained by the following:

$$\mathbf{w}_{sr}(0) = \frac{\mathbf{w}_{opt}}{\left\|\mathbf{w}_{opt}\right\|^2}, \tag{12}$$

where $\mathbf{w}_{opt}$ is the optimal weight in (7). From (6), the output square error power under the MMSE criterion of the system is obtained as

$$\xi^2_{\min} = 1 - \mathbf{w}^H\mathbf{M}\mathbf{w} = 1 - \mathbf{r}_{dx}^H\mathbf{M}^{-1}\mathbf{r}_{dx}. \tag{13}$$

In practice, one hopes to output the residual error power as small as possible to improve the STAP system performance. Signals are processed through the same non-blind array algorithm under three different array configurations. We then observe which array configuration can best upgrade system performance. The output signal-to-interference-plus-noise ratio after adaptation is given by

$$SINR = 10\log_{10}\frac{\mathbf{w}^H\mathbf{R}_{dd}\mathbf{w}}{\mathbf{w}^H\mathbf{M}\mathbf{w}}, \tag{14}$$

where $\mathbf{R}_{dd} = \mathbf{r}_{dd}\mathbf{r}_{dd}^H + \sigma_n^2\mathbf{I}$ is the desired signal

covariance matrix and $\mathbf{r}_{dd}$ represents one snapshot of the desired signal. In the following, an analytical form of the residual power is derived in order to evaluate the array configuration effect on STAP performance.

3.2. Influence of array configuration on STAP performance

In this section, the effect of array configuration on STAP system performance is analyzed. Based on the supposed prerequisite (1), it is expressed that the correlation matrix of signal $\mathbf{M}$ can be decomposed both by signal cross-correlation and auto-correlation matrix, respectively. Then we can rewrite $\mathbf{M}$ as follows:

$$\mathbf{M} = \mathbf{r}_{dd}\mathbf{r}_{dd}^H + \mathbf{r}_{dx}\mathbf{r}_{dx}^H + \sigma_n^2\mathbf{I} = \mathbf{R}_{dd} + \mathbf{r}_{dx}\mathbf{r}_{dx}^H. \quad (15)$$

Both the desired signal and noise vector are uncorrelated. According to the Sherman-Morrison-Woodbury formula [21], $\mathbf{M}^{-1}$ can be decomposed as

$$\mathbf{M}^{-1} = \mathbf{R}_{dd}^{-1} - \left(\mathbf{R}_{dd}^{-1}\mathbf{r}_{dx}\mathbf{r}_{dx}^H\mathbf{R}_{dd}^{-1} \Big/ \left(\mathbf{I} + \mathbf{r}_{dx}^H\mathbf{R}_{dd}^{-1}\mathbf{r}_{dx}\right)\right), \quad (16)$$

$\mathbf{R}_{dd}^{-1}$ can be denoted as

$$\mathbf{R}_{dd}^{-1} = \sigma_n^{-2}\left[\mathbf{I} - \mathbf{r}_{dd}\left(\mathbf{I}\sigma_n^2 + \mathbf{r}_{dd}^H\mathbf{r}_{dd}\right)^{-1}\mathbf{r}_{dd}^H\right]. \quad (17)$$

Substituting (16) and (17) into (13), we have

$$\begin{aligned}\xi_{\min}^2 &= \left(1 + \mathbf{r}_{dx}^H\mathbf{R}_{dd}^{-1}\mathbf{r}_{dx}\right)^{-1} \\ &= \left[1 + \left(\frac{\|\mathbf{r}_{dx}\|^2}{\sigma_n^2} - \frac{\mathbf{r}_{dx}^H\mathbf{r}_{dd}\left(\mathbf{I}\sigma_n^2 + \mathbf{r}_{dx}^H\mathbf{r}_{dd}\right)^{-1}\mathbf{r}_{dd}^H\mathbf{r}_{dx}}{\sigma_n^2}\right)\right]^{-1}.\end{aligned} \quad (18)$$

From (20), it is evident to see that $\xi_{\min}$ is a multivariable function of the associated array configuration parameter and some observations on the residual error power are as follows: (A1) In order to minimize the residual error power, the $\|\mathbf{r}_{dx}^H\mathbf{r}_{dd}\|$ must be minimized subject to certain value of $\|\mathbf{r}_{dx}\|$. (A2) For the case of sufficiently high input SNR, (18) can be approximated as $\mathbf{r}_{dx}^H\mathbf{R}_{dd}^{-1}\mathbf{r}_{dx} \approx \sigma_n^{-2}\|\Gamma^{\perp}\mathbf{r}_{dx}\|^2$, where $\Gamma^{\perp} = \mathbf{I} - \mathbf{r}_{dd}(\mathbf{r}_{dd}^H\mathbf{r}_{dd})^{-1}\mathbf{r}_{dd}^H$ is the orthogonal complementary projection matrix. (18) also show that the residual error power depends on the correlation between $\mathbf{r}_{dx}$ and $\mathbf{r}_{dd}$. (A3) For effectual low input SNR ($\sigma_n^2 >> \mathbf{r}_{dd}^H\mathbf{r}_{dd}$), (18) approximately becomes $\mathbf{r}_{dx}^H\mathbf{R}_{dd}^{-1}\mathbf{r}_{dx} \approx \sigma_n^{-2}\left[\|\mathbf{r}_{dx}\|^2 - \sigma_n^{-2}\|\mathbf{r}_{dx}^H\mathbf{r}_{dd}\|^2\right]$, and the residual error power in (18) becomes

$$\xi_{\min}^2 \approx \left(1 + \frac{\|\mathbf{r}_{dx}\|^2}{\sigma_n^2} - \frac{\|\mathbf{r}_{dx}^H\mathbf{r}_{dd}\|^2}{\sigma_n^4}\right)^{-1}. \quad (19)$$

From (19), it implies that the residual error power highly depends on norm of $\mathbf{r}_{dx}$ and $\|\mathbf{r}_{dx}^H\mathbf{r}_{dd}\|$. In practice, one hopes to output the residual error power as small as possible to improve the system performance. To reduce the correlation between $\mathbf{r}_{dx}$ and $\mathbf{r}_{dd}$ is one of the valid ways. The components of $\mathbf{r}_{dx}^H\mathbf{r}_{dd}$ are exactly the sidelobes of the auto-correlation and cross-correlation function of the desired signal and undesired signal (interference). The spatial-temporal channel auto-correlation function of the desired signal well describes the cross correlation between the response vectors of the components of the desired signal. The analytical forms can be obtained as follows:

$$\begin{aligned}&F_{ds}(k) \\ &= \sqrt{P_{ds}}\sum_{l=0}^{L}\left[(\mathbf{A}_d\mathbf{d}(k-1))^H\mathbf{A}\mathbf{s}(l)\right] \\ &= \sqrt{P_{ds}}\sum_{l=0}^{L}\left[\mathbf{d}^H(k-1)\mathbf{A}_d^H\mathbf{A}\mathbf{s}(l)\right] \\ &= \sqrt{P_{ds}}\sum_{l=0}^{L}\left[\begin{array}{l}\mathbf{d}^H(k-1)(\mathbf{I}_{M\times M}\otimes\mathbf{a}_{\varphi_d,\theta_d})^H \\ \bullet(\mathbf{I}_{M\times M}\otimes\mathbf{a}_{\varphi_d,\theta_d})\mathbf{s}(l)\end{array}\right] \\ &= \sqrt{P_{ds}}\sum_{m=0}^{M+L-1}\left[\mathbf{a}_{\varphi_d,\theta_d}^H\mathbf{a}_{\varphi_s,\theta_s}\mathbf{d}(k-1)\mathbf{s}(l-m)\right],\end{aligned} \quad (20)$$

where $-L \le k \le L$, and P_{ds} is the power of spatial-temporal auto-correlation. $\mathbf{A}_d$ and local replica vector $\mathbf{d}(k)$ have the same structure as $\mathbf{A}$ and $\mathbf{s}(k)$, respectively. The spatial-temporal channel cross-correlation function best depicts the cross-correlation between the response vector of the desired signal component and that of the components of the undesired signal.

$$\begin{aligned}&F_{dj}(k) \\ &= \sqrt{P_{dj}}\sum_{l=0}^{L}\left[(\mathbf{A}_d\mathbf{d}(k-1))^H\mathbf{B}_j i_j(l)\right] \\ &= \sqrt{P_{dj}}\sum_{l=0}^{L}\left[(\mathbf{d}^H(k-1)\mathbf{A}_d^H\mathbf{B}_j i_j(l)\right] \\ &= \sqrt{P_{dj}}\sum_{l=0}^{L}\left[\begin{array}{l}\mathbf{d}^H(k-1)(\mathbf{I}_{M\times M}\otimes\mathbf{a}_{\varphi_d,\theta_d})^H \\ \bullet(\mathbf{I}_{M\times M}\otimes\mathbf{a}_{\varphi_d,\theta_d})\mathbf{i}_j(l)\end{array}\right]\end{aligned}$$

$$= \sqrt{P_{dj}} \sum_{m=0}^{M+L-1} \left[\mathbf{a}_{\varphi_d,\theta_d}^H \mathbf{a}_{\varphi_j,\theta_j} \mathbf{d}(k-1)\mathbf{s}_j(l-m) \right], \quad (21)$$
$$j = 1, \cdots, j,$$

where P_{dj} denotes power of spatial-temporal cross-correlation. The relationship between $\mathbf{r}_{dx}^H \mathbf{r}_{dd}$ and the above correlation functions can be specified by the following:

$$\begin{aligned} &\left\| \mathbf{r}_{dx}^H \mathbf{r}_{dd} \right\| \\ &= F_{ds}^2(0) + \cdots + F_{ds}^2(k-1) + F_{ds}^2(k+1) + \cdots \\ &\quad + F_{ds}^2(k+L) + F_{d1}^2(0) + \cdots + F_{d1}^2(k+L) + \cdots \\ &\quad + F_{dN_j}^2(0) + \cdots + F_{dN_j}^2(k+L) \\ &= \sum_{k=-L}^{L} |F_{ds}(k)|^2 + \sum_{j=1}^{N_j} \sum_{k=-L}^{L} |F_{dj}(k)|^2 . \end{aligned} \quad (22)$$

From (20)-(22), it is observed that the spatial correlation $\mathbf{a}_{\varphi_d,\theta_d}^H \mathbf{a}_{\varphi_s,\theta_s}$, and $\mathbf{a}_{\varphi_j,\theta_j}^H \mathbf{a}_{\varphi_j,\theta_j}$, $j = 1, \cdots, j$ are important terms which can only be altered in any time-invariant environment. It is known that $\left| \mathbf{a}_{\varphi_d,\theta_d}^H \mathbf{a}_{\varphi_j,\theta_j} \right|$ and $\left| \mathbf{a}_{\varphi_d,\theta_d}^H \mathbf{a}_{\varphi_s,\theta_s} \right|$ depend on the configuration of the employed antenna array, which includes the distribution of antenna element positions, orientations, and antenna patterns. The smaller $\left| \mathbf{a}_{\varphi_d,\theta_d}^H \mathbf{a}_{\varphi_j,\theta_j} \right|$ and $\left| \mathbf{a}_{\varphi_d,\theta_d}^H \mathbf{a}_{\varphi_s,\theta_s} \right|$, the smaller $F_{ds}(k)$ and $F_{dj}(k)$, so that the smaller $\left\| \mathbf{r}_{dx}^H \mathbf{r}_{dd} \right\|$, and thus the smaller the residual error power, which leads to the better STAP performance. The same analysis results can also be applied in the scenario of multiple satellites.

3.3. Antenna array manifold vector model

From the above analysis, the better performance of the adaptive antenna under STAP can be obtained under the array configuration where $\left\| \mathbf{r}_{dx}^H \mathbf{r}_{dd} \right\|$ is minimized. The basic array configuration model consists of two parts, the element pattern and the pattern of the array with the actual elements replaced by isotropic point sources, namely array factor. The entire pattern of the array is the product of element pattern and the array factor. It consists of N omni-directional elements, equally/unequally distributed at the observation angle (φ, θ), as shown in Fig. 1(a). Figs. 1(b)-(d) shows several examples of planar arrays that are of interest. The input is a plane wave propagating in the direction with temporal frequency.

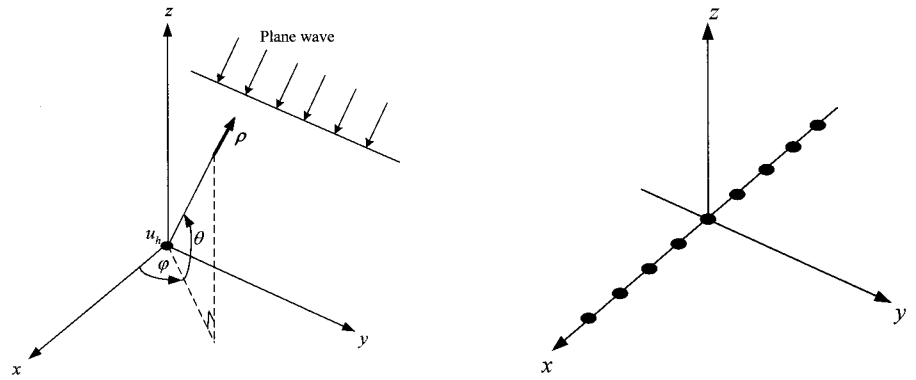

(a) Antenna array with plane wave input. (b) ULA.

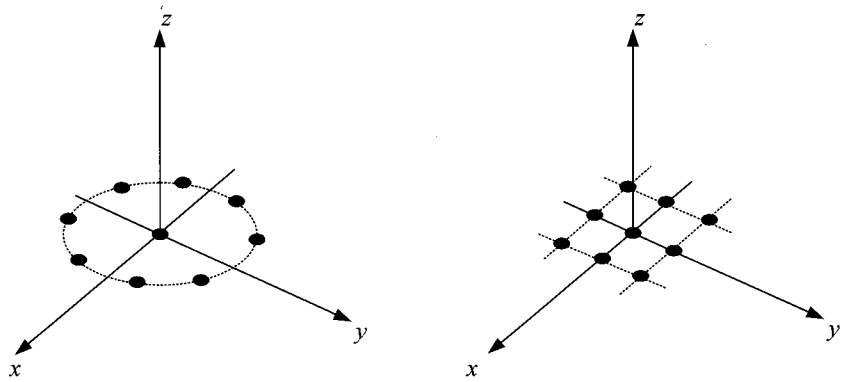

(c) UCA. (d) URA.

Fig. 1. Antenna array cartesion coordinate system and examples.

The first element is assumed to be located at the origin of the coordinate system and as the phase reference point. Therefore, the steering vector of the array is denoted as [20,22]

$$\mathbf{a}_{\varphi,\theta} = \left[e^{-j\Lambda\rho u_1} \; e^{-j\Lambda\rho u_2} \cdots e^{-j\Lambda\rho u_h} \cdots e^{-j\Lambda\rho u_N} \right]^H = \left[1 e^{-j\Lambda\rho u_2} \cdots e^{-j\Lambda\rho u_h} \cdots e^{-j\Lambda\rho u_N} \right]^H, \quad (23)$$

where $\Lambda = 2\pi / \lambda$ is the free-space wave number at some IF frequency, λ is the working wavelength,

$$\rho = [\cos(\theta)\cos(\varphi) \;\; \cos(\theta)\sin(\varphi) \;\; \sin(\theta)], \quad \theta \in [0, \pi/2], \; \varphi \in [-\pi, \pi], \quad (24)$$

ρ is a unit vector in the direction of arrival signal, and u_h is the position vector of the h^{th} array element with respect to the phase reference point, which is assumed as the origin of the orthogonal coordinate system as shown as follows:

$$u_h = [x_h \; y_h \; z_h]^H. \quad (25)$$

From (24) and (25), the inner product of ρ and u_h is

$$\rho \cdot u_h = \cos(\theta)\cos(\varphi)x_h + \cos(\theta)\sin(\varphi)y_h + \sin(\varphi)z_h. \quad (26)$$

From the discussion of previous sections, we attempt to utilize the vector model of ULA, UCA, and URA in both (20) and (21). Consequently, the corresponding $\left\| \mathbf{r}_{dx}^H \mathbf{r}_{dd} \right\|$, can be obtained. From the results of above calculations, we come to compare the resulting minimal value and the STAP performance.

4. NUMERICAL SIMULATION

4.1. Simulation parameter

In this section, computer simulations are conducted to assess the performance under different forms of antenna array configuration. For these array configurations, two scenarios of simulation are considered. All of these antenna array configurations have the same antenna elements and equally spaced array with half wavelength spacing so that the spatial aliasing is avoided and the mutual coupling effect is ignored.

In all simulation, it is performed with $N = 9$ elements in three array configurations, and with $M = 5$ taps behind each element. The one-half wavelength of radius is considered in the UCA. These scenarios encompass narrowband interference and wideband interference.

Both Tables 1 and 2 summarize the parameters in the two scenarios, respectively. In the first scenario, the received signal consists of single GPS signal (PRN30) of interest, four wideband interference (co-channel interferences; WBI), one narrowband interference (NBI), and additional white Gaussian noise. In the second scenario, the received signal consists of single GPS signal of interest, one wideband interference (co-channel interference), four narrowband interferences, and additional white Gaussian noise. In both scenarios, each of the narrowband interference has different frequency offsets relative to the L1 carrier frequency. Also, the direction of desired signal (PRN 30) is known and time between desired signal and local replica is synchronized. The *SNR* of the GPS signal is -20dB. For the tabulated parameters and with respect to different array configurations, 50 Monte Carlo simulations are performed. In each simulation, the noise and interference are generated randomly and the spatial-temporal data processing technique is used to process data and the average performance metrics are assessed. In the adaptive spatial-temporal data processing, the sampling rate is 16.368 MHz, each C/A code block lasts 1m sec, i.e., the block size is L=16368, and K=5 for block averaging. Intermediate frequency is 4.092 MHz. The length of the available data record is equal to 30ms.

Table1. Scenario 1 for single GPS signal.

Interference type	*INR* (*dB*)	*SNR* (*dB*)	Interference (φ_j, θ_j)	GPS (PRN30) (φ_s, θ_s)	Freq. offset relative to IF
WBI	10		(20°, 15°)		–
WBI	15		(50°, 50°)		–
WBI	15	–20	(45°, –30°)	(0°, 30°)	–
WBI	10		(–75°, –55°)		–
NBI	15		(–20°, –65°)		–2.8KHz

Table 2. Scenario 2 for single GPS signal.

Interference type	*INR* (*dB*)	*SNR* (*dB*)	Interference (φ_j, θ_j)	GPS (PRN30) (φ_s, θ_s)	Freq. offset relative to IF
NBI	10		(140°,20°)		–1.1KHz
NBI	15		(-50°,40°)		–1KHz
NBI	15	–20	(120°, –50°)	(0°, 30°)	–1.8KHz
NBI	10		(60°, 45°)		–3KHz
WBI	15		(–20°, –65°)		–

4.2. Simulation results

The beam pattern of the spatial-temporal weights for the three antenna configurations with half wavelength spacing is shown in Figs. 2(a), 3(a), and 4(a) for scenario 1, and in Figs. 2(b), 3(b), and 4(b) for scenario 2, which displays a well-defined null depth perfectly suppressed by the adaptive spatial-

Table 3. Antenna element $N = 9$ and $M = 5$.

	SINR improvement (dB) (average value)		
	ULA	UCA	URA
Scenario 1	38.6	40.8	42.2
Scenario 2	41.8	42.3	44.1
	MMSE Criterion (dB) (average value)		
	ULA	UCA	URA
Scenario 1	−9.1742	−11.1892	−12.0821
Scenario 2	−10.9711	−11.8892	−14.1551

temporal processing under various array configurations.

To verify the performance improvement, three same STAP systems are constructed on the three array configurations with 5 taps in each array channel. Note that MMSE value is the average result of 50 different simulations, based on the prerequisite of the same numbers and types of interference. The *SINR* improvement versus array configurations is summarized in Table 3. The *SINR* improvement is defined as the difference between the output *SINR* and input SNR. The residual error power under the MMSE criterion for ULA in Scenario 1 is −9.1742 dB, whereas −11.1892 dB for UCA, and −12.0821 dB for URA. The residual error power under the MMSE criterion for ULA in Scenario 2 is −10.9711 dB, whereas −11.8892 dB for UCA, and −14.1551 dB for URA. The average results clearly show that the use of URA can improve array output performance better than other array configurations. The effect of the number of time delay taps on interference mitigation is also analyzed. From Fig. 5, we see that, as expected, adding temporal taps does indeed improve the SINR. As can be seen from Fig. 5, the *SINR* improvement is always modest if five or more taps are employed in first scenario and eight or more taps are required in scenario 2, respectively. Nevertheless, the more the tap numbers, the longer the system computation time ($O[(NM)^2]$) and conver-gence time. In this paper, five taps are adopted for analysis.

Observe that the use of URA leads to the *SINR* improvement. In Figs. 6 and 7, the performance result for the signal correlation under different array configurations is shown. We plot the amplitudes of $F_{ds}(k)$ and $F_{dj}(k)$ in Figs. 6 and 7 for scenario 1 and scenario 2, respectively. The results demonstrate that there are no discernible difference of the correlation function peak from its correct location at zero code phase offset in Figs. 6(a) and 7(a), respectively. Even in the presence of several strong wideband or narrowband interferences, there is not a drastic broadening of the correlation function. This result meets the expectation for very large tracking errors. Small code tracking errors are defined by the

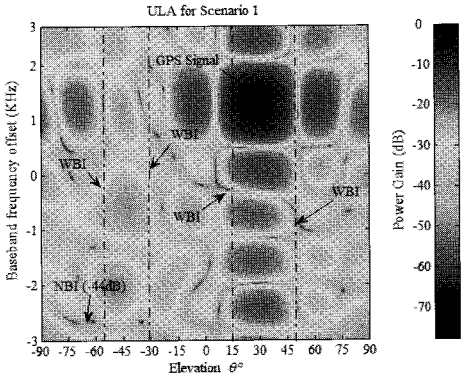

(a) Beam pattern for Scenario 1 (ULA): 4WBI, 1NBI.

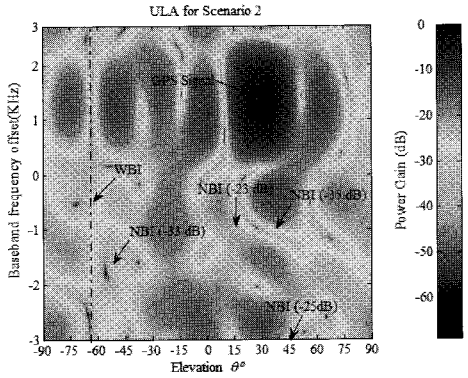

(b) Beam pattern for Scenario 2 (ULA): 4NBI, 1WBI.

Fig. 2. Antenna array pattern response.

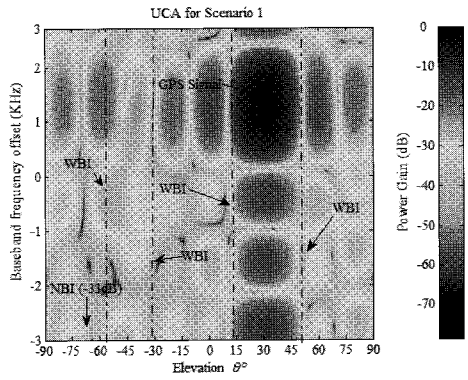

(a) Beam pattern for Scenario 1 (UCA): 4WBI, 1NBI.

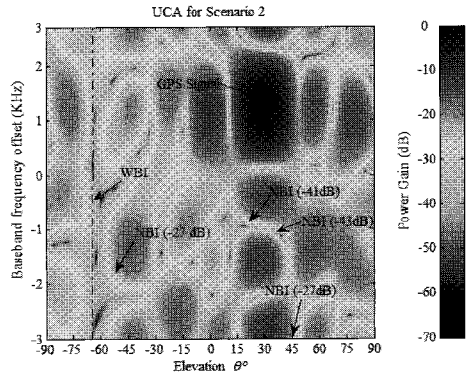

(b) Beam pattern for Scenario 2 (UCA): 4NBI, 1WBI.

Fig. 3. Antenna array pattern response.

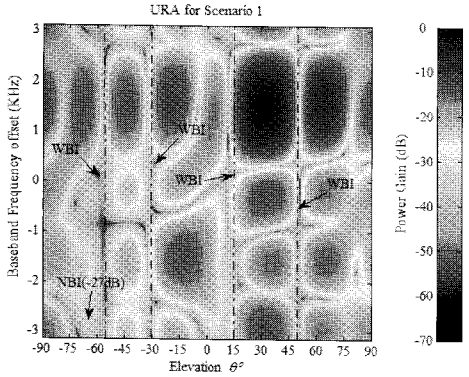

(a) Beam pattern for Scenario 1 (URA): 4WBI, 1NBI.

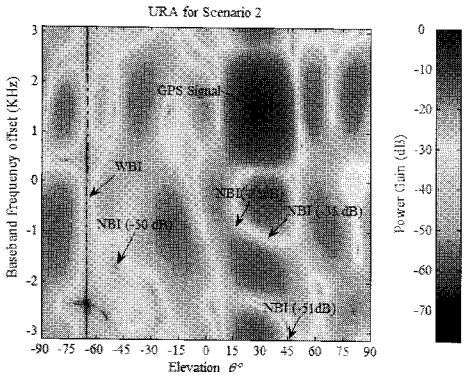

(b) Beam pattern for Scenario 2 (URA): 4NBI, 1WBI.

Fig. 4. Antenna array pattern response.

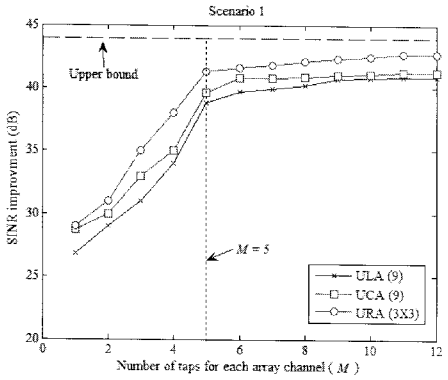

(a) Scenario 1.

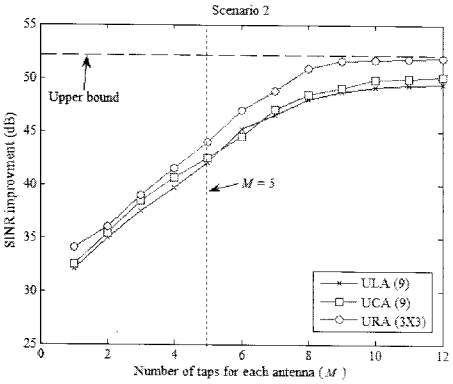

(b) Scenario 2.

Fig. 5. Number of taps v.s SINR improvement.

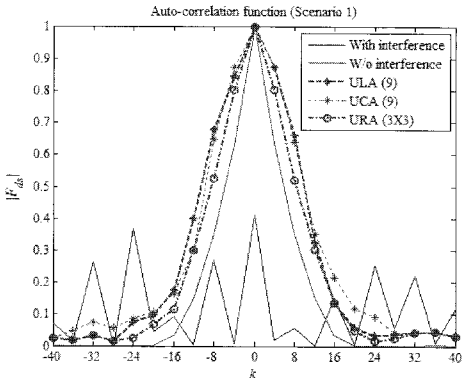

(a) auto-correlation function.

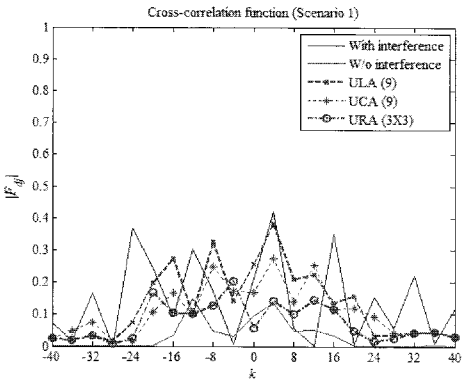

(b) cross-correlation function.

Fig. 6. Scenario 1.

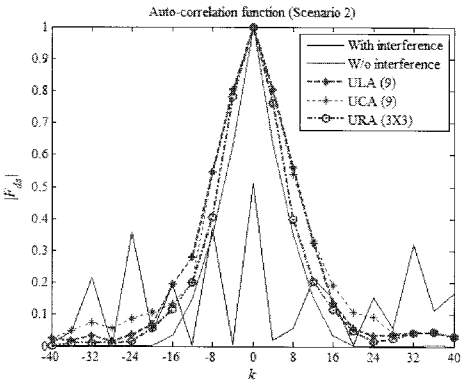

(a) auto-correlation function.

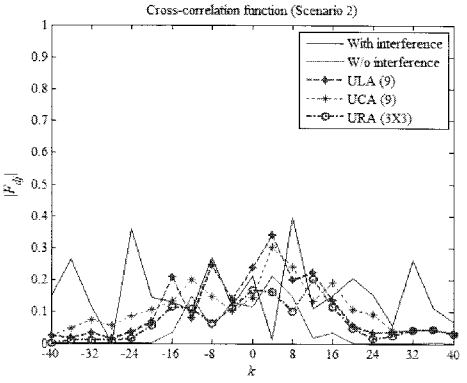

(b) cross-correlation function.

Fig. 7. Scenario 2.

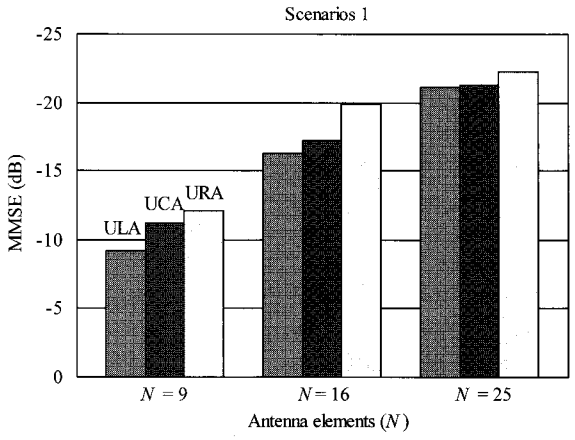

(a) Scenario 1.

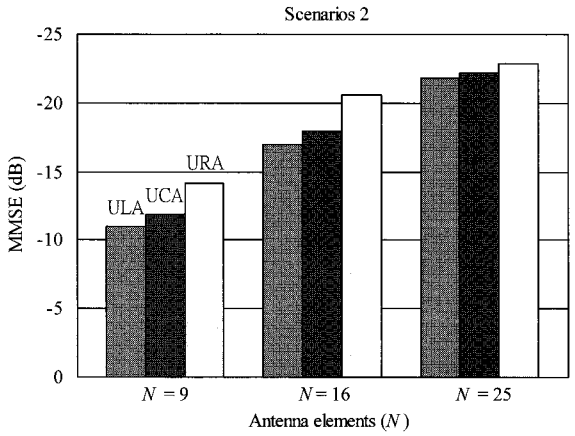

(b) Scenario 2.

Fig. 8. MMSE in dB.

shift and variance of the correlator in S-curve position. Figs. 6(b) and 7(b) tell the fact that under URA, the sidelobe levels of the associated correlation functions are reduced in comparison with that of other array configuration. Therefore, the increase in pseudo-range error is limited.

In addition, we attempt to add antenna numbers to observe its effect on STAP performance. To satisfy the square configuration of URA, 16 as well as 25 antennas are also adopted to proceed with simulation, the results of which are shown in Figs. 8(a) and (b).

These figures illustrate that adding antenna numbers does enhance STAP performance. It is also shown that the URA configuration in general has a better performance in interference mitigation. However, to constitute a URA configuration, the antenna numbers are confined to 2×2, 3×3, 4×4, etc, as opposed to ULA and UCA. When the antenna number and cost are to be considered, the UCA configuration appears to yield a better balance.

5. CONCLUSIONS

In this paper, a non-blind STAP is adopted for interference mitigation. A criterion function is developed to assess the STAP performance in various array configurations. The performance improvement of the STAP system based on different array configurations is analyzed. Also, the associated spatial-temporal correlation function through 50 different simulations of GPS orbit in interfered environment under various array configurations is assessed and compared. The performance of the STAP system is illustrated via computer simulations in scenarios with WBI, NBI, and noise. The presented approach can serve as a tool in assessing the antenna array configuration design in interference mitigation.

The analysis discussed in this paper is based on the prerequisite of equal spacing of each antenna. In the future, we will focus on the scenario of unequal spacing and design the best array configuration to reduce the effect of cross-coupling and interference. Future researches will also address the generalization of the proposed approach to account for the mitigation of multipath effect in positioning and attitude determination [23].

REFERENCES

[1] E. D. Kaplan and C. J. Hegarty, *Understanding GPS: Principle and Application*, 2nd ed., Artech House, Boston, USA, 2006.

[2] B. W. Parkinson and J. J. Spilker, *Global Positioning System: Theory and Applications*, American Institute of Aeronautics and Astronautics, Washington, USA, 1996.

[3] P. Ward, "Effects of RF interference on GPS satellite signal receiver tracking," in E. D. Kaplan (ed.) *Understanding GPS: Principles and Applications*, Artech House, Norwood, USA, pp. 209-236, 1996.

[4] J. J. Jr. Spilker and F. D. Natali, "Interference effects and mitigation techniques," in B. W. Parkinson *et al.* (eds.) *Global Positioning System: Theory and Applications*, American Institute of Aeronautics and Astronautics, Washington, USA, pp. 717-772, 1996.

[5] C. L. Chang, J. C. Juang, and Y. L. Tsai, "Development of neural network-based GPS anti-jam techniques," *Proc. of CACS Automatic Control Conf.*, Changhua, Taiwan, pp. 1076-1081, March 2004.

[6] J. W. Ketchum and J. G. Proakis, "Adaptive algorithm for estimating and suppressing narrow-band interference in PN spread-spectrum systems," *IEEE Trans. on Communications*, vol. 30, no. 5, pp. 913-924, April 1982.

[7] J. C. Juang, C. L. Chang, and Y. L. Tsai, "An interference mitigation approach against pseudolite," *Proc. of the International Symposium on GNSS/GPS*, pp. 144-156, Sydney, December 2004.

[8] D. J. Moelker, E. van der Pol, and Y. Bar-Ness,

"Adaptive antenna arrays for interference cancellation in GPS and GLONASS receivers," *Proc. of the IEEE Position, Location and Navigation Symposium*, pp. 191-198, April 1996.

[9] J. C. Juang and C. L. Chang, "Performance analysis of GPS pseudolite interference mitigation using adaptive spatial beamforming," *Proc. of the ION Annual Meeting*, pp. 1179-1187, Boston, June 2005.

[10] M. D. Zoltowski and A. S. Aecan, "Advanced adaptive null steering concepts for GPS," *Proc. of the IEEE Military Communication Conf.*, vol. 3, pp. 1214-1218, November 1995.

[11] Y. T. J. Morton, L. L. Liou, D. M. Lin, J. B. Y. Tsui. and Q. Zhou, "Interference cancellation using power minimization and self-coherence properties of GPS signals," *Proc. of the ION GNSS*, pp. 132-143, Long Beach, September 2004.

[12] W. L. Myrick, J. S. Goldstein, and M. D. Zoltowski, "Low complexity anti-jam space-time processing for GPS," *Proc. of the IEEE International Conf. on Acoustics, Speech and Signal Processing*, pp. 2233-2236, Salt Lake City, May 2001.

[13] T. K. Sarkar and R. Adve, "Space-time adaptive processing using circular arrays," *IEEE Antennas and Propagation Magazine*, vol. 43, no. 1, pp. 138-143, February 2001.

[14] P. Xiong, J. M. Michael, and N. B. Stella, "Spatial and temporal processing for global navigation satellite system: The GPS receiver paradigm," *IEEE Trans. on Aerospace and Electronic Systems*, vol. 39, no. 4, pp. 1471-1484, September 2003.

[15] R. L. Fante and J. J. Vaccaro, "Wideband cancellation of interference in a GPS receiver array," *IEEE Trans. on Aerospace and Electronic Systems*, vol. 36, no. 2, pp. 549-564, April 2000.

[16] C. L. Chang and J. C. Juang, "Analysis of spatial and temporal adaptive processing for GNSS interference mitigation," *Proc. of the International Symposium on IAIN/GNSS*, Jeju, Korea, October 2006.

[17] H. C. Lin, "Spatial correlation in adaptive arrays," *IEEE Trans. on Antennas Propagation*, vol. 30, no. 2, pp. 212-223, March 1982.

[18] Y. Zhang, K. Hirasawa, and K. Fujimoto, "A design method of linear adaptive arrays," *Proc. of the International Symposium on Antennas and Propagation*, Tokyo, pp. 333-336, August 1989.

[19] K. Yang, Y. Zhang, and Y. Mizuguchi, "Space-time adaptive processing based on unequally spaced antenna arrays," *Proc. of the 51st IEEE Vehicular Technology Conf.*, vol. 2, pp. 1220-1224, Tokyo, May 2000.

[20] H. L. Van Trees, *Optimum Array Processing*, Wiley, New York, USA, 2002.

[21] G. H. Golub and C. F. Van Loan, *Matrix Computations*, 2rd ed., Johns Hopkins University Press, Baltimore, USA, 1989.

[22] R. J. Mailloux, *Phased Array Antenna Handbook*, Artech House, Massachusetts, Norwood, USA, 1994.

[23] E. Lee, S. Chun, Y. J. Lee, T. Kang, G.-I. Jee, and J. Kim, "Parameter estimation for multipath error in GPS dual frequency carrier phase measurements using unscented Kalman filters," *International Journal of Control, Automation, and Systems*, vol. 5, no. 4, pp. 388-396, 2007.

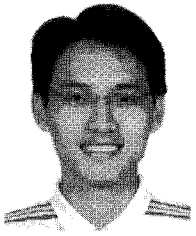

Chung-Liang Chang received the B.S. degree in Industrial Education from the National Taiwan Normal University, Taipei, Taiwan, in 1998, and the M.S. and Ph.D. degrees in Electrical Engineering from the National Cheng Kung University, Tainan, Taiwan, in 2004 and 2008, respectively. His main research interests include adaptive filtering, anti-jam techniques, array signal processing, and GNSS signal simulation.

Jyh-Ching Juang received the B.S. degree in Control Engineering and M.S. degree in Electronics from National Chiao-Tung University, HsinChu, Taiwan, in 1980 and 1982, respectively, and the Ph.D. degree in Electrical Engineering from University of Southern California, Los Angeles, USA in 1987. He is currently a Professor at the Department of Electrical Engineering, National Chyydyeng Kung University, Tainan, Taiwan. His research interests include DSP-based control applications, GPS navigation design, sensor network, and advanced signal processing.